Intraprocedural assessment of ablation margins using computed tomography co-registration in hepatocellular carcinoma treatment with percutaneous ablation
IAMCOMPLETE study

Hendriks, Pim; van Dijk, Kiki M.; Boekestijn, Bas; Broersen, Alexander; van Duijn-de Vreugd, Jacoba J.; Coenraad, Minneke J.; Dijkstra, Jouke; de Geus-Oei, Lioe Fee; Burgmans, Mark C.; More Authors

DOI
10.1016/j.diii.2023.07.002

Publication date
2023

Document Version
Final published version

Published in
Diagnostic and Interventional Imaging

Citation (APA)
Hendriks, P., van Dijk, K. M., Boekestijn, B., Broersen, A., van Duijn-de Vreugd, J. J., Coenraad, M. J., Dijkstra, J., de Geus-Oei, L. F., Burgmans, M. C., & More Authors (2023). Intraprocedural assessment of ablation margins using computed tomography co-registration in hepatocellular carcinoma treatment with percutaneous ablation: IAMCOMPLETE study. *Diagnostic and Interventional Imaging*, *105*(2), 57-64. https://doi.org/10.1016/j.diii.2023.07.002

Diagnostic and Interventional Imaging 105 (2024) 57–64

Original article/*Interventional imaging*

Intraprocedural assessment of ablation margins using computed tomography co-registration in hepatocellular carcinoma treatment with percutaneous ablation: IAMCOMPLETE study

Pim Hendriks[a,*], Kiki M van Dijk[a], Bas Boekestijn[a], Alexander Broersen[b], Jacoba J van Duijn-de Vreugd[a], Minneke J Coenraad[c], Maarten E Tushuizen[c], Arian R van Erkel[a], Rutger W van der Meer[a], Catharina SP van Rijswijk[a], Jouke Dijkstra[b], Lioe-Fee de Geus-Oei[a,d,e], Mark C Burgmans[a]

[a] *Department of Radiology, Leiden University Medical Center, 2333 ZA, Leiden, the Netherlands*
[b] *LKEB Laboratory of Clinical and Experimental Imaging, Department of Radiology, Leiden University Medical Center, 2333 ZA, Leiden, the Netherlands*
[c] *Department of Gastroenterology and Hepatology, Leiden University Medical Center, 2333 ZA Leiden, the Netherlands*
[d] *Biomedical Photonic Imaging Group, TechMed Centre, University of Twente, 7522 NB, Enschede, the Netherlands*
[e] *Department of Radiation Science & Technology, Delft University of Technology, 2628 CD, Delft, the Netherlands*

ARTICLE INFO

Keywords:
Ablation margin
Computed tomography
Thermal ablation
Hepatocellular carcinoma
Image processing

ABSTRACT

Purpose: The primary objective of this study was to determine the feasibility of ablation margin quantification using a standardized scanning protocol during thermal ablation (TA) of hepatocellular carcinoma (HCC), and a rigid registration algorithm. Secondary objectives were to determine the inter- and intra-observer variability of tumor segmentation and quantification of the minimal ablation margin (MAM).
Materials and methods: Twenty patients who underwent thermal ablation for HCC were included. There were thirteen men and seven women with a mean age of 67.1 ± 10.8 (standard deviation [SD]) years (age range: 49.1–81.1 years). All patients underwent contrast-enhanced computed tomography examination under general anesthesia directly before and after TA, with preoxygenated breath hold. Contrast-enhanced computed tomography examinations were analyzed by radiologists using rigid registration software. Registration was deemed feasible when accurate rigid co-registration could be obtained. Inter- and intra-observer rates of tumor segmentation and MAM quantification were calculated. MAM values were correlated with local tumor progression (LTP) after one year of follow-up.
Results: Co-registration of pre- and post-ablation images was feasible in 16 out of 20 patients (80%) and 26 out of 31 tumors (84%). Mean Dice similarity coefficient for inter- and intra-observer variability of tumor segmentation were 0.815 and 0.830, respectively. Mean MAM was 0.63 ± 3.589 (SD) mm (range: -6.26 −6.65 mm). LTP occurred in four out of 20 patients (20%). The mean MAM value for patients who developed LTP was -4.00 mm, as compared to 0.727 mm for patients who did not develop LTP.
Conclusion: Ablation margin quantification is feasible using a standardized contrast-enhanced computed tomography protocol. Interpretation of MAM was hampered by the occurrence of tissue shrinkage during TA. Further validation in a larger cohort should lead to meaningful cut-off values for technical success of TA.

1. Introduction

Hepatocellular carcinoma (HCC) represents the sixth most common malignancy worldwide and the fourth most common cause of cancer-related mortality. It occurs predominantly in patients with chronic liver disease, in particular cirrhosis [1]. Thermal ablation (TA) is an effective treatment for small HCC lesions and considered the preferred modality for very early stage HCC according to the Barcelona Clinic for Liver Cancer (BCLC) guidelines [2]. For solitary lesions ≤ 2 cm, the effectiveness is equal to that of surgery but at a lower risk of

Abbreviations: BCLC, Barcelona Clinic Liver Cancer; CECT, Contrast-enhanced computed tomography; CT, Computed tomography; CTCAE, Common terminology criteria for adverse events; DoS, Degree of similarity; EASL, European Association for the Study of the Liver; eGFR, Estimated glomerular filtration rate; HCC, Hepatocellular carcinoma; ICC, Intraclass correlation coefficient; LI-RADS, Liver Imaging Reporting and Data System; LTP, Local tumor progression; MAM, Minimal ablation margin; MRI, Magnetic resonance imaging; MWA, Microwave ablation; RFA, Radiofrequency ablation; SD, Standard deviation; TA, Thermal ablation; vDSC, Volumetric Dice similarity coefficient

Trial registration number: NCT04123340

* Corresponding author.
E-mail address: p.hendriks@lumc.nl (P. Hendriks).

https://doi.org/10.1016/j.diii.2023.07.002

complications [3–6]. For lesions > 2 cm surgical resection remains the preferred treatment as local tumor progression (LTP) is more prevalent after TA with relative risk ratios of up to 1.42 [7].

The most common causes of LTP are insufficient heat propagation resulting in remaining viable tumor tissue at the peripheral parts of the tumor, heat sink due to bordering intrahepatic blood vessels, and the presence of satellite nodules [8]. In order to minimize the risk of LTP after TA, it is generally recommended to achieve a minimal ablation margin (MAM) ≥ 5 mm encompassing the tumor [9,10]. After TA, contrast-enhanced computed tomography (CECT) examination is made to determine whether complete tumor necrosis with sufficient MAM has been achieved. The evaluation is usually based on a qualitative visual interpretation of side-to-side positioned diagnostic imaging and post-ablation CECT, assisted by two-dimensional in-plane measurements using anatomical landmarks.

In an attempt to identify patients at risk of developing LTP, software-assisted ablation margin assessment is considered as a promising tool [11–17]. Such software tool objectifies the MAM by using co-registration of diagnostic and post-ablation imaging. By segmenting the tumor on the diagnostic scan and the ablation zone on post-ablation CECT, a three-dimensional volumetric analysis can be performed to determine the MAM after coregistration of the images. Multiple retrospective studies found a correlation between software-assisted ablation margins and the occurrence of LTP [11–14].

Although software-assisted MAM determination is promising, no standardized or widely validated workflow has been described yet. Co-registration of preprocedural diagnostic images with a post-ablation CECT may result in registration errors as a result of differences in patient positioning, inhalation mode and imaging modality [11]. Moreover, tumor growth in the time interval between diagnostic imaging and TA may cause overestimation of the MAM. Lastly, little is known about the robustness of the co-registration process. Dissimilarities between different operators may occur while segmenting or registering medical images. We hypothesized that standardized acquisition of pre- and post-ablation images would contribute to the efficacy of software-assisted ablation margin quantification.

The primary objective of this study was to investigate the feasibility of ablation margin quantification using a standardized CECT protocol and a rigid registration algorithm. Secondary objectives were to investigate inter- and intra-observer variability, the time needed for CT-CT co-registration, and the correlation between ablation margins and local recurrence.

2. Materials and methods

The IAMCOMPLETE study was a prospective, single-arm, single center phase II feasibility study. The study protocol was approved by the institutional medical ethical board, and informed consent was obtained from all patients. The study was registered on ClinicalTrials.gov with number NCT04123340.

2.1. Patients

Twenty patients who underwent TA for HCC were recruited for this pilot study. Eligibility for TA and study participation of all patients were discussed in a multidisciplinary tumor board meeting. Inclusion criteria were: (*i*), (very) early stage HCC according to the BCLC staging system (solitary lesion ≤ 5 cm or a maximum of 3 lesions of ≤ 3 cm each); (*ii*), general eligibility for percutaneous TA; and (*iii*), age ≥18 years. HCC was diagnosed according to European Association for the Study of the Liver (EASL) guidelines based on histology or the Liver Imaging Reporting and Data System (LI-RADS) imaging characteristics on CT or magnetic resonance imaging (MRI) [18,19]. Exclusion criteria were: (*i*), estimated glomerular filtration rate (eGFR) < 30 mL/min/1.73 m^2; (*ii*), morbid obesity (body mass index ≥ 40); (*iii*), any pulmonary condition that would be a contraindication to prolonged apnea; (*iv*), Child Pugh C liver cirrhosis; (*v*), extrahepatic metastasis; and (*vi*), uncorrectable coagulopathy. Baseline patient and tumor characteristics were pseudonymized and stored in an encrypted database.

2.2. Thermal ablation procedure

TA was performed using either radiofrequency ablation (RFA) or microwave ablation (MWA). RFA was performed using Medtronic Cool-tip (single 3 or 4 cm needles, 3 × 3 cm or 3 × 4 cm needles) with up to six needle positions and MWA using Medtronic Emprint with thermosphere technology. Factors influencing the choice of TA technique and settings included tumor size, tumor location, bordering blood vessels and operator preference. Needle positioning was performed using ultrasound guidance, ultrasound-CT/MRI fusion (General Electric LOGIC E9, General Electric) or CT-guidance.

2.3. Scanning protocol

All TA procedures were performed under general anesthesia in a procedure room using an Aquilion One™ CT scanner (Canon Medical Systems). Prior to ablation, CECT was acquired using a patient weight dependent bolus of contrast material containing 350 mg of iodine per mL (Xenetix® 350, Guerbet). The full contrast protocol is reported in Table 1. Pre-oxygenated apnea was used while scanning by disconnection of the ventilation tube just before intravenous administration of the contrast agent. CT images were acquired using Sure Start™ bolus tracking at the descending aorta with a 10- and 50 s delay for arterial and venous phases, respectively.

Immediately after TA a second CECT examination was obtained using the same scanning protocol. This CECT examination was used by the performing interventional radiologist to determine whether technical success was achieved. The ablation was considered successful when the interventional radiologist estimated that a safety margin > 5 mm was obtained based on a qualitative interpretation of the pre- and post-TA imaging. The quantitative assessment was performed after the procedure and was not used to determine the technical success per-procedurally.

2.4. Follow-up

Study participants were followed for one year after TA. The follow-up schedule was similar to all regular TA patients and consisted of blood testing (including alpha-fetoprotein) at six weeks after the procedure, complemented with imaging using CECT or MRI every 3–4 months. Adverse events were graded according to the common terminology criteria for adverse events (CTCAE) 5.0 [20].

2.5. Software-assisted ablation margin quantification

Two teams performed the software-assisted ablation margin assessment, consisting of a researcher (PH, KMvD) and a radiologist with 8 or 20 years of experience in abdominal radiology (BB, MCB). In-house developed "deLIVERed" software was used, which uses an

Table 1
Protocol of intravenous administration of iodinated contrast materials for computed tomography examination according to patient weight.

	Contrast agent		NaCl (0.9%)	
Weight (kg)	Volume (mL)	Flow (ml/s)	Volume (mL)	Flow (mL/s)
< 65	100	5.0	50	5.0
65–80	130	5.5	55	5.5
80–100	160	6.0	60	6.0
> 100	190	7.0	70	7.0

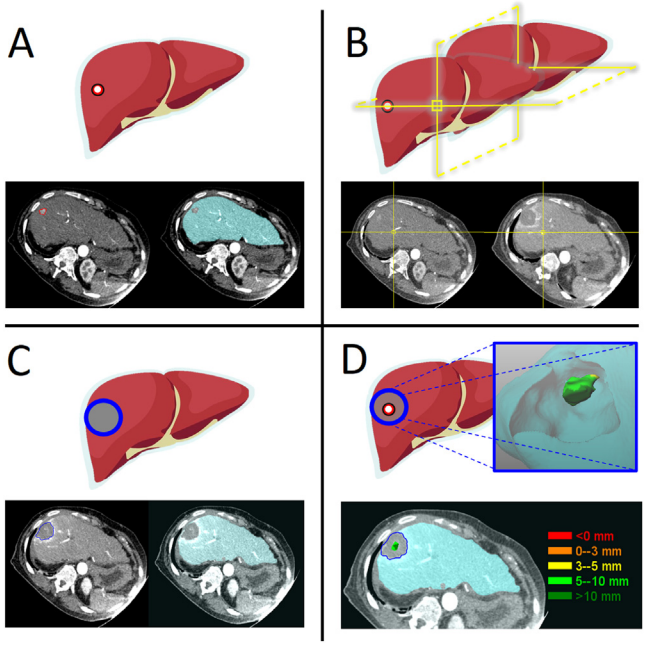

Fig. 1. Software assisted ablation margin quantification. A, *Step 1)* semiautomatic segmentation of the liver and manual segmentation of the liver tumor. B, *Step 2)* semiautomatic gray-scale based rigid registration of pre- and post-ablation computed tomography images. C, *Step 3)* semiautomatic segmentation of the ablation zone. D, *Step 4)* Analysis of quantified ablation margins.

open-source Elastix-based registration algorithm, which is implemented in MeVisLab [21,22]. Axial 1-mm slices were used for all analyses.

A schematic overview of the software assisted workflow is presented in Fig. 1. In *step 1)* semiautomatic segmentation of the liver volume on the pre-ablation scan is performed to create a "liver mask" as region of interest for image registration. Manual tumor volume segmentation was performed by segmenting the tumor contour on every axial slice. *Step 2)* consisted of a semiautomatic rigid registration of pre- and post-TA CECT. This step was aided by a projection of the "liver mask" on the post-TA CECT. After initializing the starting position of the scans onto each other (*i.e.*, dragging the liver mask onto the liver in the post-TA CECT), the automatic rigid registration algorithm was used. This result could be refined with help of anatomical landmarks or manual adjustments by means of translation and rotation. Local optimized registration was strived for in the region of the tumor and TA zone. *Step 3)* was to semi-automatically define the "liver mask" on the post-TA CECT and to semi-automatically segment the ablation necrosis on the post-TA CECT. This was done by manual segmentation of the ablation zone on multiple slices and interpolation between these contours on intermediate slices. *Step 4)* was to transform the contours and registration into a three-dimensional model that was saved as a mesh structure in a Visualization ToolKit (VTK) file. This file was then quantitatively analyzed using Paraview 5.10.0 software. A lookup table was created in which the MAM (*i.e.*, the shortest distance between the tumor surface and ablation necrosis surface) was stored. The exported lookup table was used for further statistical analysis. All steps were repeated for every tumor. The segmented liver mask on post-TA CT ensured the MAM to always represent the shortest distance from pre-ablation tumor segmentation to post-TA viable liver tissue [13].

2.6. Image analysis

MAM quantification using the previously described workflow was performed for each tumor separately in both imaging phases. Moreover, all MAM quantifications were repeated by both teams to determine intra-observer variability. The anatomical tumor side of the MAM was captured. A minimal time interval of two weeks between the two analyses was taken into account. The time needed to complete several steps of the workflow (*i.e.*, liver segmentation, tumor segmentation, co-registration and post-TA image analysis) was recorded. For inter-observer variability, the second analyses of both teams were used.

2.7. End points

The primary endpoint of this study was met when CT-CT co-registration was feasible in ≥ 80% of all patients. This parameter was objectified using a 5-points scale. (Quality of registration: 1 = "poor"; 2 = "insufficient"; 3 = "moderate"; 4 = "good"; and 5 = "perfect"). In case of disagreement between the two teams, a consensus reading was performed. At a score of 4 or 5, the registration was considered feasible and well enough to pursue ablation margin quantification.

Secondary endpoints of this study were inter- and intra-observer agreement rates for tumor delineation and MAM measurement. The MAM was defined as the single shortest distance between the tumor volume and ablation volume. In this study the tumor volume segmented from the pre-ablation CECT and the ablation volume segmented from the post-ablation CECT were co-registered to obtain the MAM using three-dimensional, software-assisted analysis. The inter- and intra-observer agreement rates were expressed as volumetric Dice similarity coefficient (vDSC) and degree of similarity (DoS) within a two-pixel range (Fig. 2). The values from vDSC and DoS range from 0 to 1, meaning no spatial overlap and perfect agreement, respectively [23]. Values between 0.6 to 0.8 were considered to indicate substantial overlap and those between 0.8 and 1.0 to indicate almost perfect overlap, as they were derived from Kappa statistics [24]. For each lesion, a single MAM value was determined as the average value of the second measurements of both observers, on arterial phase images. For lesions that were invisible on arterial phase images, portal venous phase images were used.

All follow-up CT examinations of patients developing LTP or intrahepatic metastases were double read by two radiologists with 8 and 20 years of experience in abdominal radiology (BB, MCB). In case of disagreement, consensus was reached on the anatomical orientation of LTP with respect to the tumor necrosis. This anatomical orientation was correlated to the anatomical orientation of the MAM.

2.8. Statistical analysis

Quantitative variables data were expressed as means ± standard deviations (SD) and ranges. Categorical variables were expressed as numbers and proportions. Analyses were performed using Rstudio 1.4.1106. Inter- and intra-observer variability were analyzed using Bland Altman plots. Mean MAM-values of the two observers were

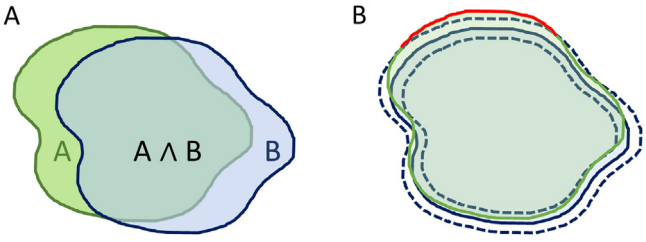

Fig. 2. Inter- and intra-observer variability outcome measures of tumor segmentation. *A)* shows the volumetric Dice similarity coefficient (vDSC), which is calculated by dividing the overlapping volume of two segmented volumes by the non-overlapping parts of these volumes. *B)* shows the degree of similarity (DoS) within 2 voxel distance between two segmentations. Dashed blue lines represent 2 voxel distance of the blue segmentation and the green segmentation exceeds this margin for approximately 20% at the top border (in red).

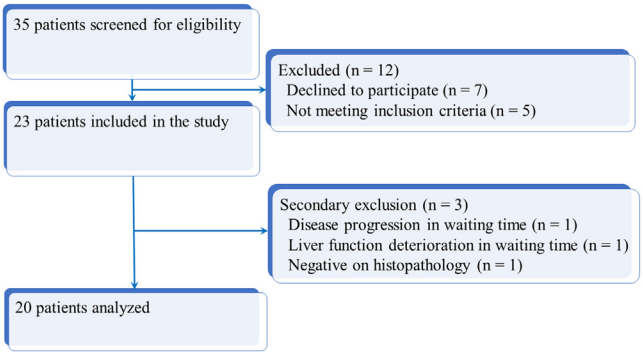

Fig. 3. Flowchart of the study population.

plotted in box-plots and expressed as medians with inter quartile ranges. The intraclass correlation coefficient (ICC) for inter-observer variability was determined [25].

3. Results

Informed consent was obtained from 23 patients, of whom 20 patients were treated according to the study protocol (Fig. 3). Reasons for preliminary exclusion were lack of histopathological confirmation of HCC after a combined biopsy and TA procedure for a LI-RADS-4 lesion (n = 1) [19], disease progression to Child-Pugh C liver cirrhosis (n = 1) or to intermediate HCC (n = 1) within a maximum of six weeks waiting time. Table 2 shows the baseline characteristics of the patients analyzed. A total of 20 patients with 31 HCC lesions were included with a mean lesion diameter of 18.8 ± 7.34 mm [SD] (range: 8–38 mm). Eight patients underwent prior HCC treatment before inclusion in this study.

Thirteen patients were treated with MWA and seven patients with RFA. TA was deemed successful with sufficient ablation margins in 30/31 ablations by discretion of the treating physician based on side-to-side reading of pre- and post-ablation CECT. In those patients, no additional ablation was performed. In one patient a CTCAE 5.0 grade 3 bleeding occurred that led to preliminary termination of the procedure. In this patient additional TA was performed in a second treatment. Other adverse events were CTCAE 5.0 grade 3: post-procedural pleural effusion (n = 1), grade 2: hematoma formation (n = 2), grade 2: postprocedural pain (n = 2), grade 2: postprocedural fever (n = 1), and grade 1: iatrogenic vascular thrombosis of a segmental vessel leading to segmental liver infarction (n = 1).

Fig. 4 shows two examples of MAM quantification. Table 3 shows HCC lesion visibility on the different CT imaging phases and ablation margin quantification parameters. Out of 31 lesions, 18 lesions were visible on both CT phases and 11 lesions were visible on one CT phase only. Two solitary lesions in two different patients were not visible on both CT phases and therefore not suitable for analysis. These lesions were targeted by fusion of ultrasound images and MR images. The total time for tumor segmentation, scan registration and ablation zone segmentation was 19 min 31 s ± 6 min 39 s (SD) (range: 07 min

Table 2
Characteristics of 20 patients with hepatocellular carcinomas treated with thermal ablation.

Variable		Value
Age (year)		67.1 ± 10.8 [49.1–81.1]
Sex		
	Male	13 (65%)
	Female	7 (35%)
Cirrhosis		
	Yes	17 (85%)
	No	3 (15%)
Etiology of cirrhosis		
	Hepatitis B	1 (6%)
	Hepatitis C	1 (6%)
	Alcohol abuse	14 (82%)
	NASH	1 (6%)
Child-Pugh score	A	12 (88%)
	B	5 (12%)
BCLC stage		
	Very early	8 (40%)
	Early	10 (50%)
	Intermediate	2 (10%)
Diagnostic imaging		
	CT	9 (45%)
	MRI	11 (55%)
Prior HCC treatment		
	None	11 (60%)
	Surgical resection	1 (5%)
	RFA	4 (20%)
	TACE	4 (20%)
Number of HCC lesions		
	1	13 (70%)
	2	5 (20%)
	3	1 (5%)
	4	0 (0%)
	5	1 (5%)
Lesion size (mm)		18.8 ± 7.3 [8.0–38.0]
Ablation technique		
	RFA	7 (35%)
	MWA	13 (65%)

BCLC = Barcelona Clinic for Liver Cancer, CT = computed tomography; HCC = hepatocellular carcinoma; MWA = microwave ablation; MRI = magnetic resonance imaging; NASH = non-alcoholic steatohepatitis; RFA = radiofrequency ablation; TACE = trans-arterial chemoembolization.
Quantitative data are reported as means ± standard deviations; numbers into brackets are ranges. Qualitative variables are expressed as raws numbers followed by percentages into parentheses.

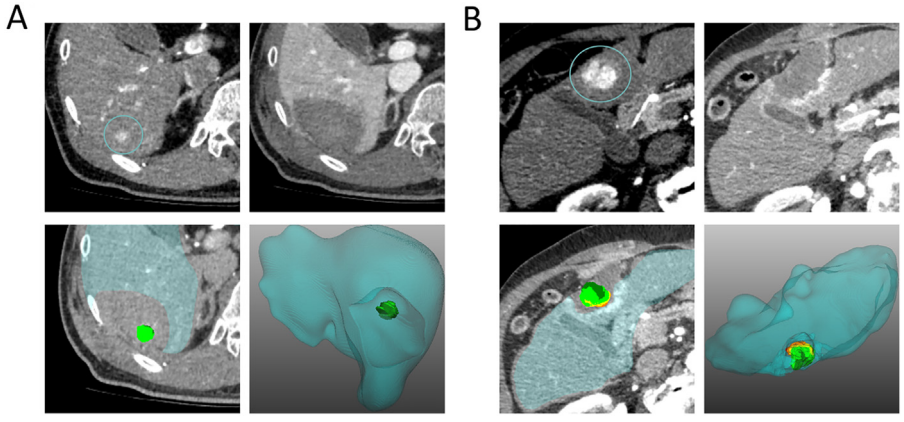

Fig. 4. Two examples of minimal ablation margin quantification of thermal ablation of hepatocellular carcinoma lesions, using in-house built software. A) Small lesion is segment 6 of the liver with an ablation zone > 5 mm. B) large lesion in segment 4 of the liver with 0 mm of minimal ablation margin.

Table 3
Ablation margin quantification parameters.

Variable	Results
Visibility of HCC on CT phase	
Arterial and portal venous phases	18 (58%)
Portal venous phase only	6 (19%)
Arterial phase only	5 (16%)
Invisible	2 (6%)
Duration for delineation (min:s)	
Tumor	04:28 ± 01:57 [01:13–11:00]
Ablation zone	04:06 ± 01:53 [01:16–11:29]
Registration	06:55 ± 03:38 [01:44–19:12]
Total	19:31 ± 06:39 [07:36–36:01]
Minimal ablation margin (vDSC)	
Arterial phase	0.728 ± 3.349 [−5.834–6.203]
Portal venous phase	0.554 ± 3.749 [−7.567–10.666]
Total	0.626 ± 3.589 [−7.567–10.666]

Quantitative data are reported as means ± standard deviations; numbers into brackets are ranges. Qualitative variables are expressed as raw numbers followed by percentages into parentheses.
CT = computed tomography; HCC = hepatocellular carcinoma; vDSC = volumetric Dice similarity coefficient.

36 s–36 min 01 s) (Table 3). vDSC rates of inter- and intra-observer variability for tumor segmentation were 0.815 ± 0.069 (SD) (range: 0.660–0.930) and 0.830 ± 0.073 (SD) (range: 0.512–0.930), respectively (Table 4). The mean MAM was 0.63 ± 3.59 (SD) mm (range: −7.57–10.67 mm). For individual lesions that were visible on both CT phases, a mean volumetric difference of 31.8% between both CT phases was found. However, there was no uniformity in whether delineation in arterial or portal-venous phase resulted in a larger tumor volume.

Two lesions in two patients were invisible on both arterial and portal venous phases, which made them infeasible for ablation margin quantification. In another three lesions in two patients, the registration quality was insufficient (with scores of 3/5, 3/5 and 2/5) to accurately quantify the ablation margins, resulting in a total feasibility of 26/31 (84%) lesions in 16/20 (80%) patients. For the feasible lesions, Bland Altman analysis revealed a mean absolute error between the two observers of 2.15 ± 2.12 mm [SD] (range: 0.39 −10.45 mm) for ablation margin quantification, with an ICC of 0.794 (95% confidence interval: 0.594–0.895) (Fig. 5).

Four patients developed LTP in one of the ablated tumors. This included the single patient in whom the thermal ablation was technically unsuccessful but terminated due to a bleeding. In one patient, the tumor was invisible on ultrasound and pre-ablation CECT. This lesion was targeted using fusion navigation of ultrasound and diagnostic MRI. The mean MAM of the other two lesions that developed LTP was −4.00 mm, compared to an overall mean MAM of 0.626 ± 3.589 (SD) mm (range: −6.26–6.65 mm) (Fig. 6). Noteworthy, three patients who developed LTP were treated for recurrent HCC as part of this study. Moreover, three lesions were peripherally located in the liver dome. Six patients developed new HCC lesions elsewhere in the liver. None of the patients with a MAM > 0 mm developed LTP. In the group of patients with a MAM < 0 mm, 2/9 (22%) patients developed LTP.

4. Discussion

Quantitative ablation margin analysis using co-registration imaging is a promising method to assess technical success of liver tumor TA and has the potential to be superior to visual qualitative assessment [11–14]. Our study demonstrates that a standardized imaging protocol with intraprocedural pre- and post-TA CT under general anesthesia with preoxygenated breath hold allows accurate image co-registration. We found a feasibility for accurate co-registration of pre- and post-TA CECT examinations in 80% of patients and 83.9% of all lesions treated, using the standardized scanning protocol.

In previous retrospective studies on ablation margin quantification, exclusion rates up to 40% were reported, when co-registration of diagnostic CECT or MRI with post-TA CECT was used [11,14,26,27]. Reasons for inaccurate co-registration in these studies included differences in the position and shape of the liver as a result of differences in patient positioning and breathing mode, and motion artifacts. Feasibility rates similar to ours were found in a study that used intraprocedural pre- and post-ablation CECT, after selection of well demarcated HCC lesions [12]. Standardization of pre- and post-TA CECT protocols thus seem to contribute to the feasibility of ablation margin quantification.

As secondary endpoints, we investigated inter- and intra-observer variability of segmentation of the tumor. Reproducibility of segmentation is a prerequisite for accurate quantitative ablation margin analysis. We found high inter- and intra-observer vDSC rates for tumor segmentation. Although the vDSC is an objective measure of volumetric overlap, it is less sensitive in larger volumes [28]. The DoS within a 2-voxel distance contributes to an objective measure for inter- and intra-observer agreement, as it is volume independent. With DoS values of 0.781 ± 0.140 [SD] (range: 0.536–0.978) and 0.828 ± 0.120 [SD] (range: 0.526–0.982) at a voxel size of $0.71 \times 0.71 \times 1\ mm^3$, high inter- and intra-observer agreement rates were found. In a recent systematic review on ablation margin quantification by Minier et al., only a limited number of studies evaluated inter- and intra-operator characteristics of segmentation or MAM quantification [29]. Most studies used Kappa statistics, and therefore categorized the outcome measure to < 0 mm, 0–5 mm and > 5 mm. Values ranged from 0.68 to >0.95. Kim et al. reported a Kappa of 0.71 for inter-observer agreement of HCC delineation, resulting in a few recommendations for optimization, which were partly implemented in our study (small slice thickness < 3 mm, respiratory motion restriction, multiphasic CT, and consensus meeting for overcoming discrepancies) [30]. Using MRI examinations with larger voxel sizes,

Table 4
Results of inter- and-intra observer variability in hepatocellular carcinoma delineation on the different imaging phases.

Variable	Results	
	vDSC	DoS
Inter-observer variability in tumor delineation		
Arterial phase	0.816 ± 0.085 [0.608–0.910]	0.782 ± 0.161 [0.454–0.997]
Portal venous phase	0.811 ± 0.087 [0.580–0.930]	0.780 ± 0.163 [0.379–0.959]
Total	0.815 ± 0.069 [0.660–0.930]	0.781 ± 0.140 [0.536–0.978]
Intra-observer variability in tumor delineation		
Arterial phase	0.823 ± 0.061 [0.665–0.920]	0.840 ± 0.088 [0.653–0.979]
Portal venous phase	0.837 ± 0.085 [0.512–0.930]	0.815 ± 0.143 [0.526–0.982]
Total	0.830 ± 0.073 [0.512–0.930]	0.828 ± 0.120 [0.526–0.982]

Quantitative data are reported as means ± standard deviations; numbers into brackets are ranges. vDSC= volumetric Dice similarity coefficient. DoS = degree of similarity (chances of two delineations to overlap within a 2 voxel distance).

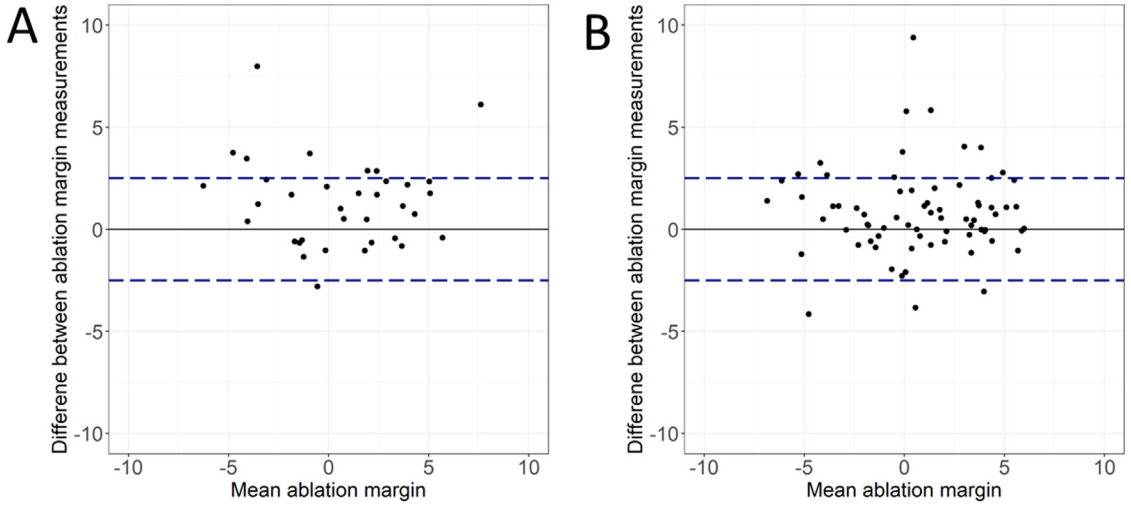

Fig. 5. Bland-Altman plots for A) inter-observer variability and B) intra-observer variability of ablation margin quantification. X-axis shows the mean of the two measurements of quantified ablation margins and the Y-axis shows the difference between the two measurements. The blue dashed lines depict the mean inter-observer difference of 2.5 mm. The mean absolute error between two observers was 2.15 ± 2.12 mm [SD] (range: 0.39–10.45 mm).

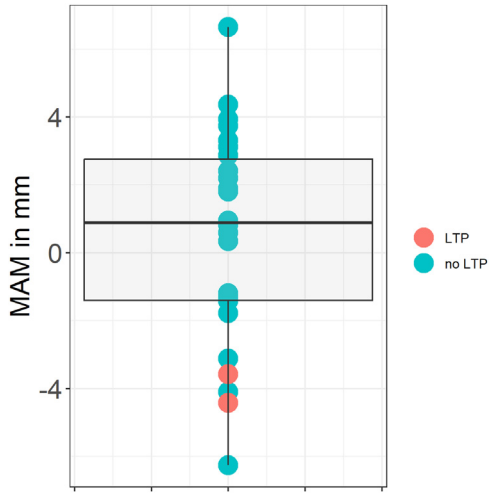

Fig. 6. Boxplot of minimal ablation margins (MAM) for ablated lesions that developed local tumor progression (LTP) (n = 2) vs those that did not develop LTP (n = 26).

Hocquelet et al. found DSC values > 0.9 for each lesion in ablation margin quantification, [31]. In our study, we found a mean difference in tumor volume of 31% between segmentations of the same tumor in arterial phase and portal venous phases. This is an important factor to take into account when interpreting the result of quantitative margin analysis. CT level and window settings may influence the volumetric measurements when segmenting a tumor [32]. Other factors that may influence tumor segmentation are the timing of image acquisition, contrast volume and contrast load. Optimized scan timing, standardized CT level and window settings, target segmentation training, and consensus reading may contribute to the robustness of the workflow [33].

In our study, a mean MAM of 0.626 ± 3.589 [SD] mm (range: −6.26–6.65 mm) was found, with 36.5% of all MAM quantifications being < 0 mm. This was considerably lower than the intended ablation margin of at least 5 mm. Despite the limited ablation margin, the LTP rates were in concordance with that of an earlier study in a similar population [34]. Other studies on quantitative ablation margin analyses also found margins that were considerably lower than 5 mm [12–14]. Although a MAM of > 5 mm is associated with good clinical outcomes, this may often not be achieved in practice. Previous studies reported a MAM > 5 mm in only 2.7% [12] and 37.5% of lesions where they used software-assisted ablation margin quantification [14]. In one study, the overestimation of qualitative interpretation of TA was shown, as the number of patients requiring additional TA increased from 12/150 to 35/150 after introducing software-assisted quantification of MAM with a threshold of 2 mm [35]. In our study, LTP occurred in only 2/9 patients with a quantified MAM <0 mm. There may be several explanations for this. Experimental studies have demonstrated that considerable tissue shrinkage may occur during TA [36,37]. As a result of the contraction of the ablated tissue, the volume of the ablation zone may be smaller than the tumor volume as determined on the pre-procedural scan, even in a patient in whom the tumor was completely ablated with sufficient margins. Tissue shrinkage may vary considerably depending on individual patient and tumor characteristics, as well as the TA equipment and settings. Also, it occurs non-uniform over time and asymmetrical [38]. Moreover, the software may incorrectly calculate a negative MAM as a result of errors in image co-registration or segmentation of the tumor and/or ablation zone. In fact, our study demonstrates that segmentation is subject to inter- and intra-observer variability, and may be discordant between arterial and portal venous phases. Future research should focus on methods to further reduce such variability to increase reliability and reproducibility of ablation margin quantification, preferably with fast, reliable and fully automated co-registration and segmentation. It is important to stress that a negative MAM does not necessarily mean that a tumor was incompletely ablated as it is only investigated as a predictive factor. On the other hand, none of the patients in our study with a positive MAM-value developed LTP, and a positive MAM value should of course be aimed for.

In this study, a rigid registration algorithm was used for performing quantitative margin assessment. Previous research showed that non-rigid deformations may be present in the liver, especially caused by breathing motion differences [29,39]. Non-rigid registration allows for transformation and scaling of images rather than just translation and rotation to reach an optimal registration [40]. Since the process of TA actually causes local deformation of the tissue, non-rigid algorithms should be restricted in order not to overcompensate for local deformations [41]. Using the standardized intraprocedural scanning protocol with ventilation tube disconnection, the main reason for large deformation (breathing motion and positioning artifacts) were prevented and fast rigid registration with high accuracy was feasible.

Limitations of this feasibility study were the limited number of included patients, the retrospective use of ablation margin quantification software and the limited number of events, which brings limitations to statistical analysis on the MAM results. Despite these limitations we have been able to prospectively demonstrate a feasible pipeline for robust ablation margin quantification.

In conclusion, ablation margin quantification after TA of HCC can be made by implementing a standardized scanning protocol consisting of pre- and post-ablation CECT under breath hold by disconnection of the ventilation tube under general anesthesia. High inter- and intra-observer agreement rates were found for lesion delineation. LTP seemed to be associated with low MAM values (*i.e.*, < 0 mm), but this should further be studied in larger cohort trials.

Human rights

The authors declare that the work described has been performed in accordance with the Declaration of Helsinki of the World Medical Association revised in 2013 for experiments involving humans.

Informed consent and patient details

The authors declare that they obtained a written informed consent from the patients included in the article. The authors declare that this report does not contain any personal information that could lead to the identification of the patients.

Funding

This study received no specific funding.

Author contributions

All authors attest that they meet the current International Committee of Medical Journal Editors (ICMJE) criteria for Authorship.

Declaration of Competing Interest

The authors have no conflicts of interest related to this work to declare.

CRediT authorship contribution statement

Pim Hendriks: Conceptualization, Methodology, Validation, Formal analysis, Investigation, Data curation, Writing – original draft, Visualization. **Kiki M van Dijk:** Validation, Investigation, Writing – original draft. **Bas Boekestijn:** Formal analysis, Investigation, Writing – review & editing. **Alexander Broersen:** Methodology, Software, Investigation, Data curation, Writing – review & editing, Supervision. **Jacoba J van Duijn-de Vreugd:** Resources, Data curation. **Minneke J Coenraad:** Resources, Writing – review & editing. **Maarten E Tushuizen:** Resources, Writing – review & editing. **Arian R van Erkel:** Conceptualization, Resources, Writing – review & editing. **Rutger W van der Meer:** Conceptualization, Resources, Writing – review & editing. **Catharina SP van Rijswijk:** Conceptualization, Resources, Writing – review & editing. **Jouke Dijkstra:** Conceptualization, Software, Writing – review & editing, Supervision. **Lioe-Fee de Geus-Oei:** Methodology, Writing – review & editing, Supervision. **Mark C Burgmans:** Conceptualization, Methodology, Validation, Investigation, Resources, Data curation, Writing – review & editing, Visualization, Supervision.

References

[1] Forner A, Reig M, Bruix J. Hepatocellular carcinoma. Lancet 2018;391:1301–14.
[2] Reig M, Forner A, Rimola J, Ferrer-Fàbrega J, Burrel M, Garcia-Criado Á, et al. BCLC strategy for prognosis prediction and treatment recommendation: the 2022 update. J Hepatol 2022;76:681–93.
[3] Cho YK, Kim JK, Kim WT, Chung JW. Hepatic resection versus radiofrequency ablation for very early stage hepatocellular carcinoma: a Markov model analysis. Hepatology 2010;51:1284–90.
[4] Cucchetti A, Piscaglia F, Cescon M, Colecchia A, Ercolani G, Bolondi L, et al. Cost-effectiveness of hepatic resection versus percutaneous radiofrequency ablation for early hepatocellular carcinoma. J Hepatol 2013;59:300–7.
[5] Izumi N, Hasegawa K, Nishioka Y, Takayama T, Yamanaka N, Kudo M, et al. A multicenter randomized controlled trial to evaluate the efficacy of surgery vs. radiofrequency ablation for small hepatocellular carcinoma (SURF trial). J Clin Oncol 2019;37:4002.
[6] Doyle A, Gorgen A, Muaddi H, Aravinthan AD, Issachar A, Mironov O, et al. Outcomes of radiofrequency ablation as first-line therapy for hepatocellular carcinoma less than 3 cm in potentially transplantable patients. J Hepatol 2019;70:866–73.
[7] Xu X-L, Liu X-D, Liang M, Luo B-M. Radiofrequency ablation versus hepatic resection for small hepatocellular carcinoma: systematic review of randomized controlled trials with meta-analysis and trial sequential analysis. Radiology 2018;287:461–72.
[8] Habibollahi P, Sheth RA, Cressman ENK. Histological correlation for radiofrequency and microwave ablation in the local control of hepatocellular carcinoma before liver transplantation: a comprehensive review. Cancers 2020;13:104.
[9] Crocetti L, de Baere T, Pereira PL, Tarantino FP. CIRSE standards of practice on thermal ablation of liver tumours. Cardiovasc Intervent Radiol 2020;43:951–62.
[10] Nakazawa T, Kokubu S, Shibuya A, Ono K, Watanabe M, Hidaka H, et al. Radiofrequency ablation of hepatocellular carcinoma: correlation between local tumor progression after ablation and ablative margin. AJR Am J Roentgenol 2007;188:480–8.
[11] Hendriks P, Noortman WA, Baetens TR, van Erkel AR, van Rijswijk CSP, van der Meer RW, et al. Quantitative volumetric assessment of ablative margins in hepatocellular carcinoma: predicting local tumor progression using nonrigid registration software. J Oncol 2019;2019:4049287.
[12] Laimer G, Schullian P, Jaschke N, Putzer D, Eberle G, Alzaga A, et al. Minimal ablative margin (MAM) assessment with image fusion: an independent predictor for local tumor progression in hepatocellular carcinoma after stereotactic radiofrequency ablation. Eur Radiol 2020;30:2463–72.
[13] Sandu RM, Paolucci I, Ruiter SJS, Sznitman R, de Jong KP, Freedman J, et al. Volumetric quantitative ablation margins for assessment of ablation completeness in thermal ablation of liver tumors. Front Oncol 2021;11:6230.
[14] Kim YS, Lee WJ, Rhim H, Lim HK, Choi D, Lee JY. The minimal Ablative margin of radiofrequency ablation of hepatocellular carcinoma (>2 and < 5cm) needed to prevent local tumor progression: 3D quantitative assessment using CT image fusion. AJR Am J Roentgenol 2010;195:758–65.
[15] Takeyama N, Mizobuchi N, Sakaki M, Shimozuma Y, Munechika J, Kajiwara A, et al. Evaluation of hepatocellular carcinoma ablative margins using fused pre- and post-ablation hepatobiliary phase images. Abdom Radiol 2019;44:923–35.
[16] Tomonari A, Tsuji K, Yamazaki H, Aoki H, Kang J-H, Kodama Y, et al. Feasibility of fused imaging for the evaluation of radiofrequency ablative margin for hepatocellular carcinoma. Hepatol Res 2013;43:728–34.
[17] An C, Jiang Y, Huang Z, Gu Y, Zhang T, Ma L, et al. Assessment of ablative margin after microwave ablation for hepatocellular carcinoma using deep learning-based deformable image registration. Front Oncol 2020;10:573316.
[18] European Association for the Study of the Liver. EASL clinical practice guidelines: management of hepatocellular carcinoma. J Hepatology 2018;69:182–236.
[19] Chernyak V, Fowler KJ, Kamaya A, Kielar AZ, Elsayes KM, Bashir MR, et al. Liver Imaging Reporting and Data System (LI-RADS) version 2018: imaging of hepatocellular carcinoma in at-risk patients. Radiology 2018;289:816–30.
[20] Freites-Martinez A, Santana N, Arias-Santiago S, Viera A. Using the common terminology criteria for adverse events (CTCAE - version 5.0) to evaluate the severity of adverse events of anticancer therapies. Actas Dermosifiliogr 2021;112:90–2.
[21] Shamonin D, Bron E, Lelieveldt B, Smits M, Klein S, Staring M. Fast parallel image registration on CPU and GPU for diagnostic classification of Alzheimer's disease. Front Neuroinform 2014;7.
[22] Klein S, Staring M, Murphy K, Viergever MA, Pluim JPW. Elastix: a toolbox for intensity-based medical image registration. IEEE Trans Med Imaging 2010;29:196–205.
[23] Zou KH, Warfield SK, Bharatha A, Tempany CM, Kaus MR, Haker SJ, et al. Statistical validation of image segmentation quality based on a spatial overlap index. Acad Radiol 2004;11:178–89.
[24] McHugh ML. Interrater reliability: the kappa statistic. Biochem Med 2012;22:276–82.
[25] Benchoufi M, Matzner-Lober E, Molinari N, Jannot AS, Soyer P. Interobserver agreement issues in radiology. Diagn Interv Imaging 2020;101:639–41.
[26] Sibinga Mulder BG, Hendriks P, Baetens TR, van Erkel AR, van Rijswijk CSP, van der Meer RW, et al. Quantitative margin assessment of radiofrequency ablation of a solitary colorectal hepatic metastasis using MIRADA RTx on CT scans: a feasibility study. BMC Med Imaging 2019;19:71.
[27] Faber RA, Burghout KST, Bijlstra OD, Hendriks P, van Erp GCM, Broersen A, et al. Three-dimensional quantitative margin assessment in patients with colorectal

liver metastases treated with percutaneous thermal ablation using semi-automatic rigid MRI/CECT-CECT co-registration. Eur J Radiol 2022;156:110552.
[28] Lohmann P, Stavrinou P, Lipke K, Bauer EK, Ceccon G, Werner JM, et al. FET PET reveals considerable spatial differences in tumour burden compared to conventional MRI in newly diagnosed glioblastoma. Eur J Nucl Med Mol Imaging 2019;46:591–602.
[29] Minier C, Hermida M, Allimant C, Escal L, Pierredon-Foulongne M-A, Belgour A, et al. Software-based assessment of tumor margins after percutaneous thermal ablation of liver tumors: a systematic review. Diagn Interv Imaging 2022;103:240–50.
[30] Kim YS, Kim JW, Yoon WS, Kang MK, Lee IJ, Kim TH, et al. Interobserver variability in gross tumor volume delineation for hepatocellular carcinoma. Strahlenther Onkol 2016;192:714–21.
[31] Hocquelet A, Trillaud H, Frulio N, Papadopoulos P, Balageas P, Salut C, et al. Three-dimensional measurement of hepatocellular carcinoma ablation zones and margins for predicting local tumor progression. J Vasc Interv Radiol 2016;27:1038–45 e2.
[32] Van Hoe L, Haven F, Bellon E, Baert AL, Bosmans H, Feron M, et al. Factors influencing the accuracy of volume measurements in spiral CT: a phantom study. J Comput Assist Tomogr 1997;21:332–8.
[33] Eriksen JG, Salembier C, Rivera S, De Bari B, Berger D, Mantello G, et al. Four years with FALCON: an ESTRO educational project: achievements and perspectives. Radiother Oncol 2014;112:145–9.
[34] Burgmans MC, Too CW, Fiocco M, Kerbert AJC, Lo RHG, Schaapman JJ, et al. Differences in patient characteristics and midterm outcome between Asian and European patients treated with radiofrequency ablation for hepatocellular carcinoma. Cardiovasc Intervent Radiol 2016;39:1708–15.
[35] Shin S, Lee JM, Kim KW, Joo I, Han JK, Choi BI, Klotz E. Postablation assessment using follow-up registration of CT images before and after radiofrequency ablation (RFA): prospective evaluation of midterm therapeutic results of RFA for hepatocellular carcinoma. AJR Am J Roentgenol 2014;203:70–7.
[36] Brace CL, Diaz TA, Hinshaw JL, Lee Jr FT. Tissue contraction caused by radiofrequency and microwave ablation: a laboratory study in liver and lung. J Vasc Interv Radiol 2010;21:1280–6.
[37] Rossmann C, Garrett-Mayer E, Rattay F, Haemmerich D. Dynamics of tissue shrinkage during ablative temperature exposures. Physiol Meas 2014;35:55–67.
[38] Farina L, Weiss N, Nissenbaum Y, Cavagnaro M, Lopresto V, Pinto R, et al. Characterisation of tissue shrinkage during microwave thermal ablation. Int J Hyperthermia 2014;30:419–28.
[39] Luu HM, Moelker A, Klein S, Niessen W, van Walsum T. Quantification of nonrigid liver deformation in radiofrequency ablation interventions using image registration. Phys Med Biol 2018;63:175005.
[40] Crum WR, Hartkens T, Hill DLG. Non-rigid image registration: theory and practice. Br J Radiol 2004;77:S140–53.
[41] Dong C, Chen YW, Seki T, Inoguchi R, Lin C-L, Han X-h. Non-rigid image registration with anatomical structure constraint for assessing locoregional therapy of hepatocellular carcinoma. Comput Med Imaging Graph 2015;45:75–83.